AD-A123 706 STRUCTURE AND DYNAMICS OF THE WINTER POLAR CAP F REGION 1/1
(U) AIR FORCE GEOPHYSICS LAB HANSCOM AFB MA
J BUCHAU ET AL. 03 SEP 82 AFGL-TR-82-0258

UNCLASSIFIED F/G 4/1 NL

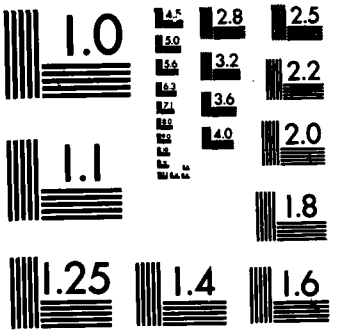

AFGL-TR-82-0258
ENVIRONMENTAL RESEARCH PAPERS, NO. 792

Structure and Dynamics of the Winter Polar Cap F Region

J. BUCHAU
B.W. REINISCH
E.J. WEBER
J.G. MOORE

3 September 1982

SPACE PHYSICS DIVISION PROJECT 4643
AIR FORCE GEOPHYSICS LABORATORY
HANSCOM AFB, MASSACHUSETTS 01731

AIR FORCE SYSTEMS COMMAND, USAF

This report has been reviewed by the ESD Public Affairs Office (PA) and is releasable to the National Technical Information Service (NTIS).

This technical report has been reviewed and is approved for publication.

Alva T Stair, Jr.

DR. ALVA T. STAIR, Jr
Chief Scientist

Qualified requestors may obtain additional copies from the Defense Technical Information Center. All others should apply to the National Technical Information Service.

Unclassified

SECURITY CLASSIFICATION OF THIS PAGE (When Data Entered)

REPORT DOCUMENTATION PAGE	READ INSTRUCTIONS BEFORE COMPLETING FORM
1. REPORT NUMBER: AFGL-TR-82-0258	2. GOVT ACCESSION NO.: AD-A123 706
	3. RECIPIENT'S CATALOG NUMBER:
4. TITLE (and Subtitle): STRUCTURE AND DYNAMICS OF THE WINTER POLAR CAP F REGION	5. TYPE OF REPORT & PERIOD COVERED: Scientific. Interim.
	6. PERFORMING ORG. REPORT NUMBER: ERP, No. 792
7. AUTHOR(s): J. Buchau, B. W. Reinisch*, E.J. Weber, J.G. Moore	8. CONTRACT OR GRANT NUMBER(s):
9. PERFORMING ORGANIZATION NAME AND ADDRESS: Air Force Geophysics Laboratory (PHY) Hanscom AFB Massachusetts 01731	10. PROGRAM ELEMENT, PROJECT, TASK AREA & WORK UNIT NUMBERS: 62101F 46430801
11. CONTROLLING OFFICE NAME AND ADDRESS: Air Force Geophysics Laboratory (PHY) Hanscom AFB Massachusetts 01731	12. REPORT DATE: 3 September 1982
	13. NUMBER OF PAGES: 29
14. MONITORING AGENCY NAME & ADDRESS(if different from Controlling Office)	15. SECURITY CLASS. (of this report): Unclassified
	15a. DECLASSIFICATION/DOWNGRADING SCHEDULE:

16. DISTRIBUTION STATEMENT (of this Report)

Approved for public release; distribution unlimited.

17. DISTRIBUTION STATEMENT (of the abstract entered in Block 20, if different from Report)

18. SUPPLEMENTARY NOTES

*University of Lowell
Center for Atmospheric Research
Lowell, MA 01854

19. KEY WORDS (Continue on reverse side if necessary and identify by block number)

Polar cap
Aurora
Ionospheric sounding

20. ABSTRACT (Continue on reverse side if necessary and identify by block number)

All-sky photometer images and ionospheric soundings taken at Thule, Greenland (86° CGL) in December 1979 and January 1982 reveal three groups of forms important in the organization of the winter polar cap ionosphere.

1) The most prominent features are sun-aligned, generally unstructured, subvisual, F-region arcs, extending for more than 1200 km (limit of all-sky camera field of view) across the polar cap. These arcs usually drift from dawn to dusk at speeds between 100 and 250 m/sec, however, stagnations of

DD FORM 1 JAN 73 1473 EDITION OF 1 NOV 65 IS OBSOLETE

Unclassified

SECURITY CLASSIFICATION OF THIS PAGE (When Data Entered)

20. Abstract (Continued)

arc drift and drift reversals have been observed. The arcs are produced by soft particle precipitation.

2) During a magnetically disturbed period the arcs disappeared and large patches of enhanced F-region ionization drifted at speeds of 250 to 700 m/sec across the field of view in the antisunward direction. Although arcs are produced by soft particle precipitation, preliminary results from the Dynamics Explorer satellite do not indicate any localized soft electron precipitation into the patches.

3) On a few occasions both forms were observed simultaneously. Between F-region sun-aligned arcs drifting from dawn to dusk, small patches of ionization were observed moving at much higher speeds in the antisunward direction.

Both the arcs and the patches appear as strong localized irregularities in the ionospheric soundings. The Doppler information provided by the Digisonde 128 PS was used to relate backscatter traces to individual arcs or patches and to track these features over more than 1500 km. Many observations suggest specular reflection from electron density enhancements associated with the optical forms, rather than scatter from field-aligned irregularities embedded in the arcs or patches. High velocities occurred more often during magnetically active periods.

F-region arcs are bands of enhanced ionization, imbedded in a background ionosphere with a base height h'F of approximately 250 km and a critical frequency of about 4 MHz (2×10^5 el/cm^3). The virtual heights in the ionograms did not change during transit of the arcs through the zenith. During the active periods, when the antisunward-moving patches were observed, the background ionization dropped to less than 3 MHz (10^5 el/cm^3) while the base height (h'F) moved up to heights above 400 km. The strongly ionized patches (foF2 more than 8 MHz) however, were observed to reach a minimum virtual range of about 250 km during the zenith transit, leading to rapid h'F fluctuations in the order of 200 km within minutes.

Preface

The authors wish to thank R. W. Gowell, J. Lloyd, and J. B. Waarama of AFGL for engineering support, and W. Whiting of Regis College and M. Shirley of the University of Lowell, for assistance in data analysis.

Flight support from the 4950th Test Wing, Wright-Patterson AFB, Ohio, is gratefully acknowledged.

Contents

Illustrations

Structure and Dynamics of the Winter Polar Cap F Region

1. INTRODUCTION

Ground based and airborne measurements of auroral emissions and ionospheric structure in the polar cap, conducted by the AFGL Airborne Ionospheric Observatory (AIO), have shown the structure and drift of polar cap F-layer auroras.[1] These initial observations on 9 and 10 December 1979 revealed a previously unreported large scale dynamic behavior of polar cap auroras; however, the total time span of the observations was less than 6.5 h, and they were made under quiet magnetic conditions (Σ Kp $\leq$ 15). To gain further insight into the occurrence conditions, dynamic behavior, and detailed structure of the polar cap F-layer, the AIO was used in a series of ground based optical and ionospheric measurements at Thule AB, Greenland (86° CGL) from 17 to 27 January 1982. Results from these measurements show three types of polar cap ionospheric structure,

(1) The most prominent features are sun-aligned, generally unstructured, sub-visual F-region arcs similar to those reported by Weber and Buchau.[1] These extend for more than 1200 km (All-Sky Imaging Photometer field of view) across the polar cap, and drift toward dusk at speeds between

(Received for publication 2 September 1982)

1. Weber, E.J., and Buchau, J. (1981) Polar cap F-layer auroras, Geophys. Res. Lett. 8:125.

100 and 250 m/sec. Drift reversals and periods of no drift have also been observed. These arcs are produced by low energy (E < 500 eV) precipitating electrons, and are characterized by intense ionospheric irregularities.

(2) During a magnetically disturbed period (Kp > 4) the arcs disappeared and large patches of luminous F-region ionization drifted in the anti-sunward direction at speeds from 250 to 700 m/sec. Preliminary comparison with the Dynamics Explorer (DE-2) low altitude plasma instrument (LAPI) data[2] shows no increase in soft electron flux above the patches.

(3) On a few occasions both forms were observed simultaneously.

In this paper we briefly describe auroral dynamics measured by an All-Sky Imaging Photometer (ASIP). These optical measurements provide a framework in which to interpret the ionospheric sounder data from the Digisonde 128 PS.

2. INSTRUMENTATION

The instrumentation used in these experiments is part of the Air Force Geophysics Laboratory's Airborne Ionospheric Observatory, an NKC 135 aircraft equipped for ionospheric, auroral, and propagation research. The experiments discussed here demonstrate the aircraft's capability to operate as a mobile ground station as well as an airborne observatory.

The ionospheric measurements were made with a Digisonde 128 PS[3] which provides standard virtual height versus frequency information, amplitude information, and, of special significance for the experiments discussed here, the determination of the predominant Doppler component in each frequency-range bin. This Doppler capability allows the identification and tracking of drifting F-layer irregularity structures in the presence of spread F. The Digisonde was operated in a mode of one ionogram every 2.5 min, providing alternating unambiguous Doppler ranges of ±11 and ±22 Hz.

The Doppler ranges were chosen (assuming reflections at frequencies up to 10 MHz), to identify speeds of irregularities of up to 1000 km/h uniquely. Such speeds have been reported as typical for convective drift of the polar cap F-region plasma.[4, 5]

2. Winningham, J.D., and Sharber, J. (1982) Private communication.

3. Bibl, K., and Reinisch, B.W. (1978) The universal digital ionosonde, Radio Sci. 13:519.

4. Heelis, R.A., and Hanson, W.B. (1980) High latitude ion convection in the nighttime F region, J. Geophys. Res. 85:1995.

5. Heppner, J.P., Miller, M.L., Pongratz, M.B., Smith, G.M., Smith, L.L., Mende, S.B., and Natch, N.R. (1981) The cameo barium releases: $E_{||}$ fields over the polar cap, J. Geophys. Res. 86:3519.

The aircraft standard three-wire HF antenna[6] was used for transmission and reception, precluding any directional measurements.

Optical measurements were made with the ASIP,[7, 8] which provides the capability of monitoring weak auroral features at four different wavelengths, with 30 sec time resolution for each wavelength. Measurements for the polar cap experiments were made using 25 Å interference filters to measure λ6300 (O I), 4278 (N_2+), 5577 (O I), and 5200 (N I). Only the 6300 Å measurements will be discussed in this paper.

3. OPTICAL OBSERVATIONS

The three types of auroral structure described in the Introduction are shown schematically in Figure 1. The figure shows the Corrected Geomagnetic Latitude (CGL) and Local Time (CGLT) distribution of arcs (Type 1), patches (Type 2), and arcs and patches (Type 3). Also shown is the ASIP field of view (assumed emission height of 250 km) for 06 CGLT to illustrate the area of the polar cap visible from Thule.

Figure 2 shows a sequence of 6300 Å ASIP images at 10-min intervals on 9 December 1979 to illustrate the Type 1 structure. The noon-midnight (12-00) and dawn-dusk (06-18) meridians were projected into the 155° field-of-view image for an assumed height of 250 km. The intersection of these lines is the north CG pole. At about 2120 UT, sun-aligned arcs appeared along the top and bottom horizons of the images. The bright area near the zenith is the Milky Way. From 2120 until 2203 UT (image not shown) the arcs drifted from dusk toward dawn. This is best seen in the movement of the arc at the bottom horizon toward the zenith. At 2203 UT, both arcs simultaneously reversed direction and began to drift from dawn to dusk. Multiple arc structures drifted into the ASIP field of view from the dawn horizon for the remainder of the observing period. During the 3 h of observations the arcs remained generally sun-aligned.

Figure 3 shows a sequence of 6300 Å images on 22 January 1982 at 3-min intervals, to illustrate the Type 2 (drifting patch) structure. The first image at 1003 UT shows a total absence of polar cap arc structure over the entire ASIP field of view. The bright glow along the noon horizon is the poleward edge of the

6. Gowell, R.W., and Whidden, R.W. (1968) Ionospheric Sounders in Aircraft, AFCRL-TR-68-0369, AD 678047.

7. Mende, S.B., Eather, R.H., and Aamodt, E.K. (1977) Instrument for the monochromatic observation of all sky auroral images, Appl. Opt. 16:1691.

8. Weber, E.J., Buchau, J., Eather, R.H., and Lloyd, J.W.F. (1977) Large Scale Optical Mapping of the Ionosphere, AFGL-TR-77-0236, AD A051122.

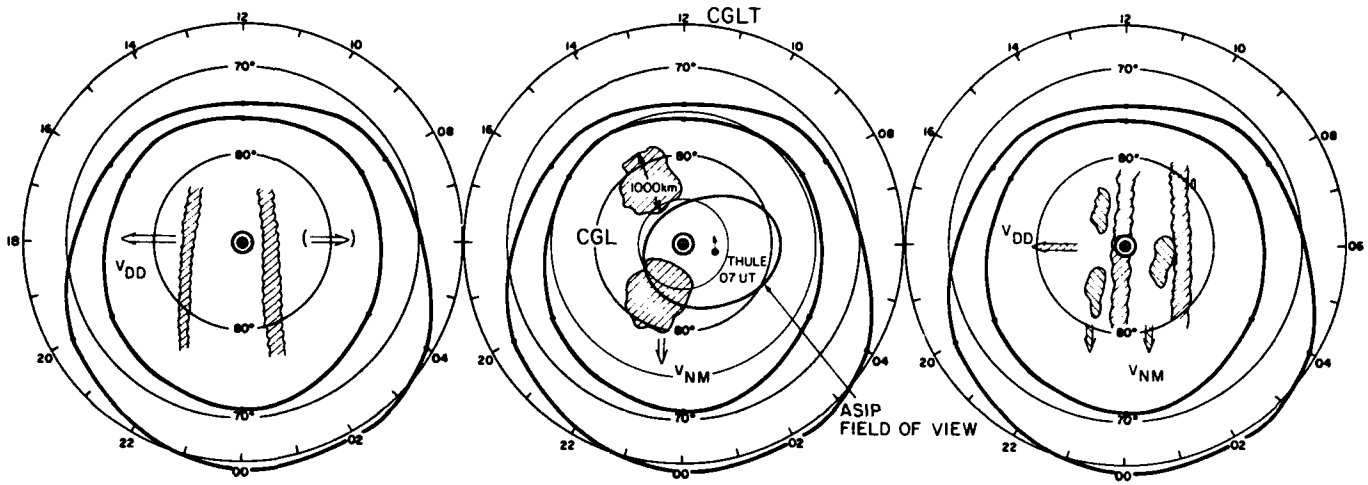

Figure 1. Three Types of Polar Cap F-Region Structures Observed

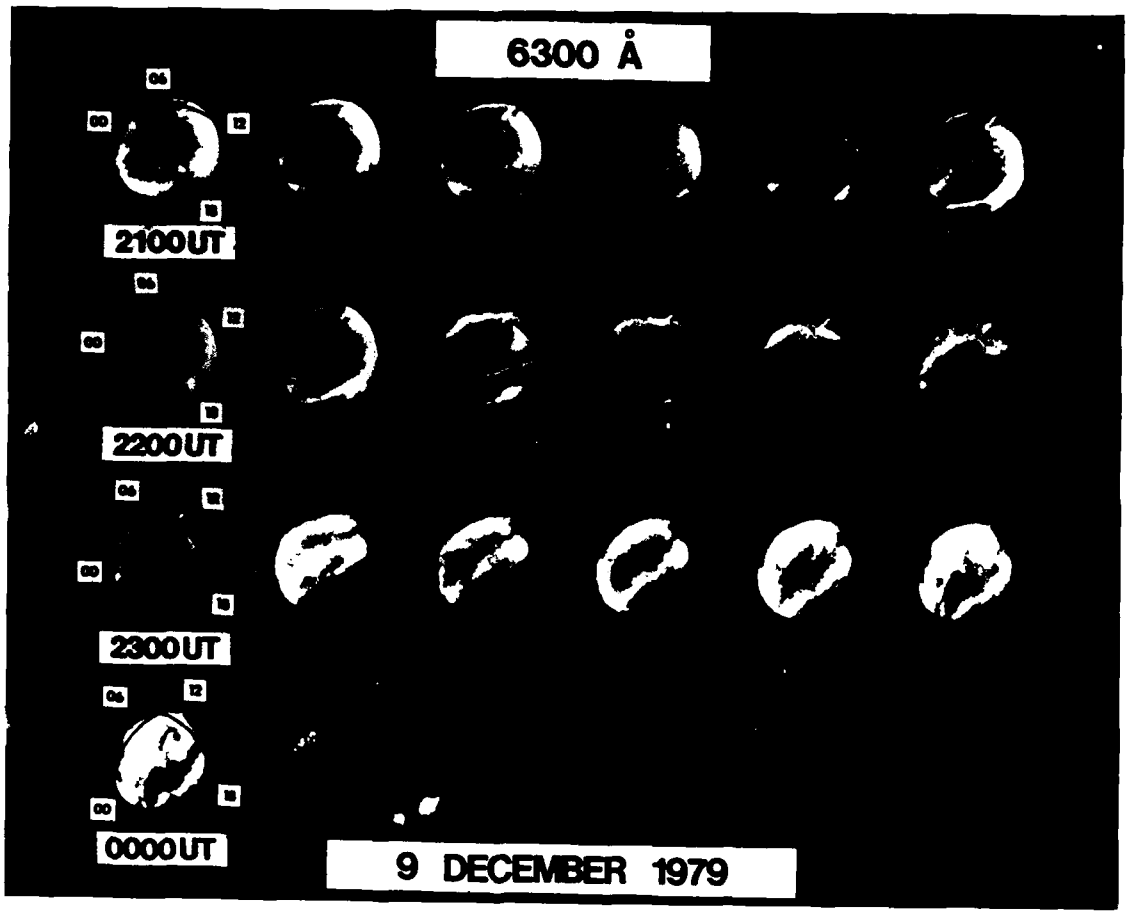

Figure 2. All-Sky Imaging Photometer Images Taken at 10-min Intervals on 9 Dec 1979, Showing Sun-Aligned Arcs (Type 1)

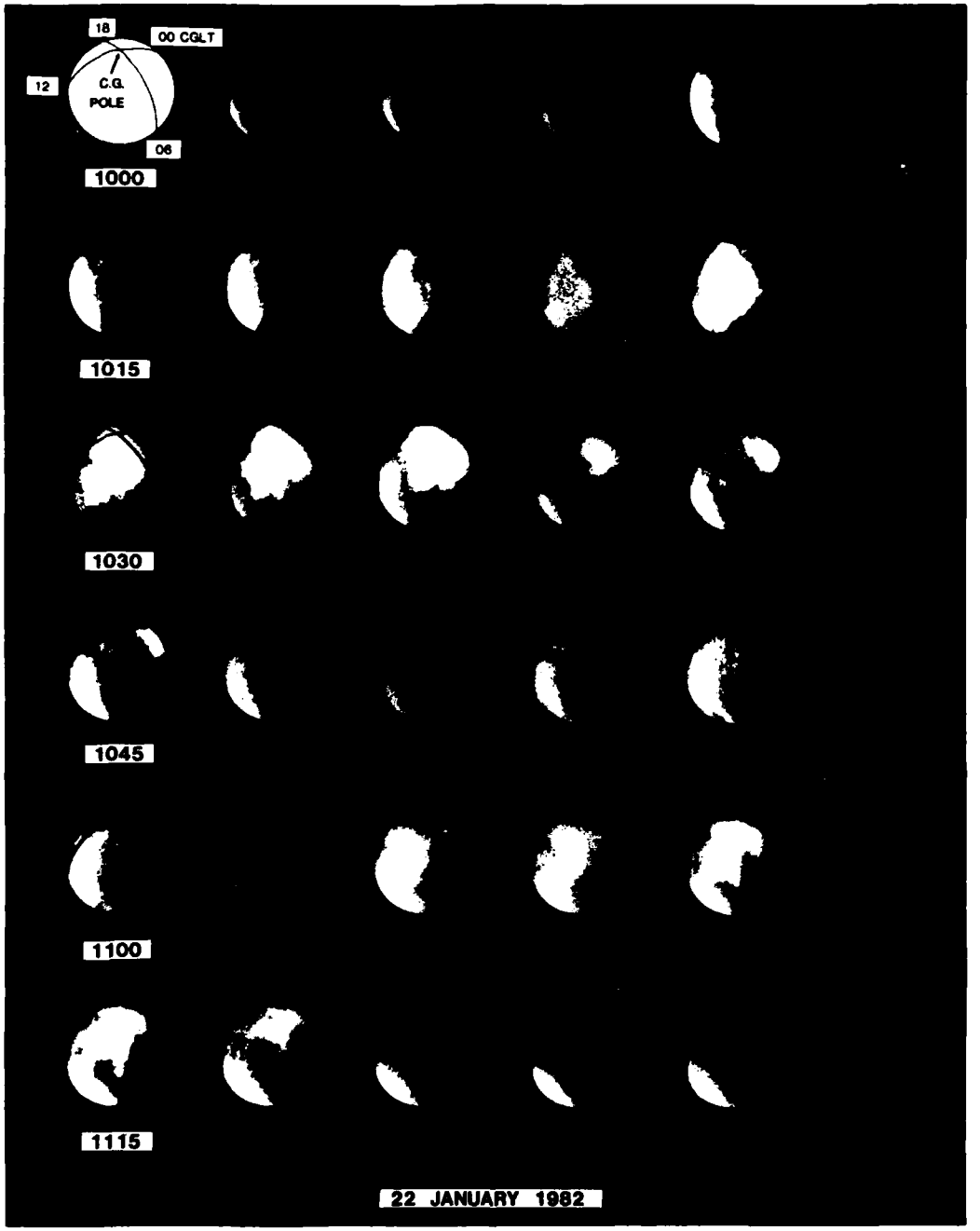

Figure 3. All-Sky Imaging Photometer Images Taken at 3-min Intervals on 22 Jan 1982, Showing Patches (Type 2)

dayside cusp region located near 79° CGL. Between 1021 and 1024 UT, a bright patch can be resolved as it moves away from the noon horizon. The patch, of ~1000 km in extent, drifted through the zenith (1030 UT) in the antisunward direction. A second patch that exhibited similar behavior drifted through the zenith at ~1121 UT.

The glow on the horizon toward noon is interpreted as the poleward edge of the dayside cusp aurora. At these local times, the solar elevation angle varied from -20° to -17.5°, and no twilight enhancement in the zenith is expected. Thus, the drifting patches appear to originate in the dayside cusp region, and are observed to drift over and beyond the CG pole toward midnight.

An example of the less frequently observed Type 3 structure (arcs and patches) is shown in Figure 4. This figure shows 6300 Å images at 5-min intervals from 2255 to 2330 UT on 24 January 1982. At 2300 UT, three sun-aligned arcs are visible: one along the dawn horizon, one through the zenith, and one along the dusk horizon. During the 35-min period shown, the three arcs drifted slowly toward dusk. A patch developed adjacent to the arc through the zenith

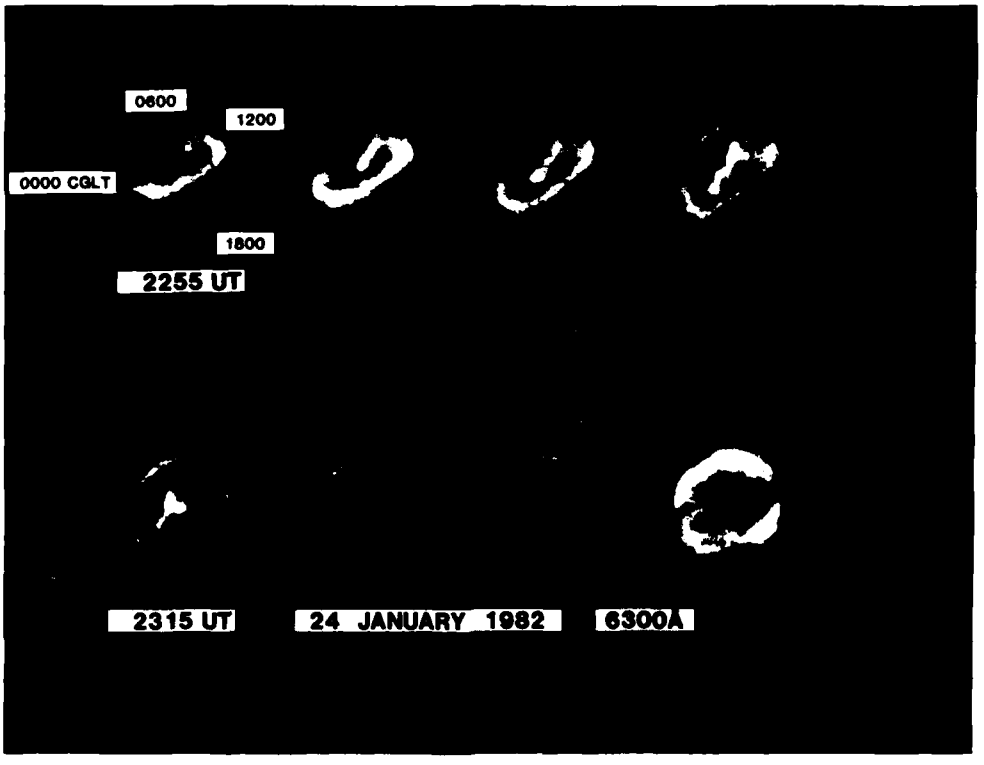

Figure 4. All-Sky Imaging Photometer Images Taken at 5-min Intervals on 24 Jan 1982, Showing Arcs and Small Patches (Type 3)

and drifted along the arc in the anti-sunward direction. This type of structure was observed on other occasions and is easily seen in the 16 mm movie format. However, the patches are often short lived, and are difficult to display in the montage presentation.

4. IONOSPHERIC SOUNDINGS

4.1 Virtual Height/Range Observations of Drifting Arcs

Throughout the observing period, ionospheric soundings were made with the aircraft's Digisonde 128 PS at a rate of one ionogram per 2.5 min. An example of a digital amplitude ionogram typical for periods of steady arc drift over the observing station (the aircraft is stationed on the ground at Thule) is shown in the lower right section of Figure 5. The amplitudes are printed out using an optically weighted font,[3] which preserves digital information while providing the appearance of a normal analog (amplitude) ionogram.

The ionogram shows the overhead ionosphere under strong spread F conditions, with a critical frequency of 4 MHz (estimate). Also present are two large irregularities at virtual ranges of approximately 400 and 450 km. The upper right panel (labeled STATUS) is a presentation of the Doppler frequency measured in each frequency-range bin, printed out only where significant amplitudes (those shown in the panel below) are present. Doppler frequency numbers (Doppler bin numbers) 1 to 7 indicate positive Doppler, 8 to 15 negative Doppler, both increasing with increasing numerical value. Since numbers ≥ 8 are darker than numbers 1 to 7, negative Doppler areas appear dark, while positive Doppler areas, especially those showing small positive velocities, appear gray. Two regions of negative Doppler (O and A) and two regions of positive Doppler (B and C) are identifiable. A separation of the status ionogram into a negative and a positive Doppler ionogram is shown in the top left and bottom left panels of Figure 5, respectively. Here the numbers have a potential range of 1 to 15 and again indicate increasing Doppler with increasing numerical value. These panels show spread F returns from the overhead ionosphere (marked O) with a slightly negative Doppler of less than 1 Hz at 4 MHz. The speed of the vertical motion of the overhead ionosphere can be estimated, using the Doppler relation for radar returns

$$v = \frac{d}{2f} \times c_o = \frac{d}{f} \times 150 \text{ m/sec} \qquad (1)$$

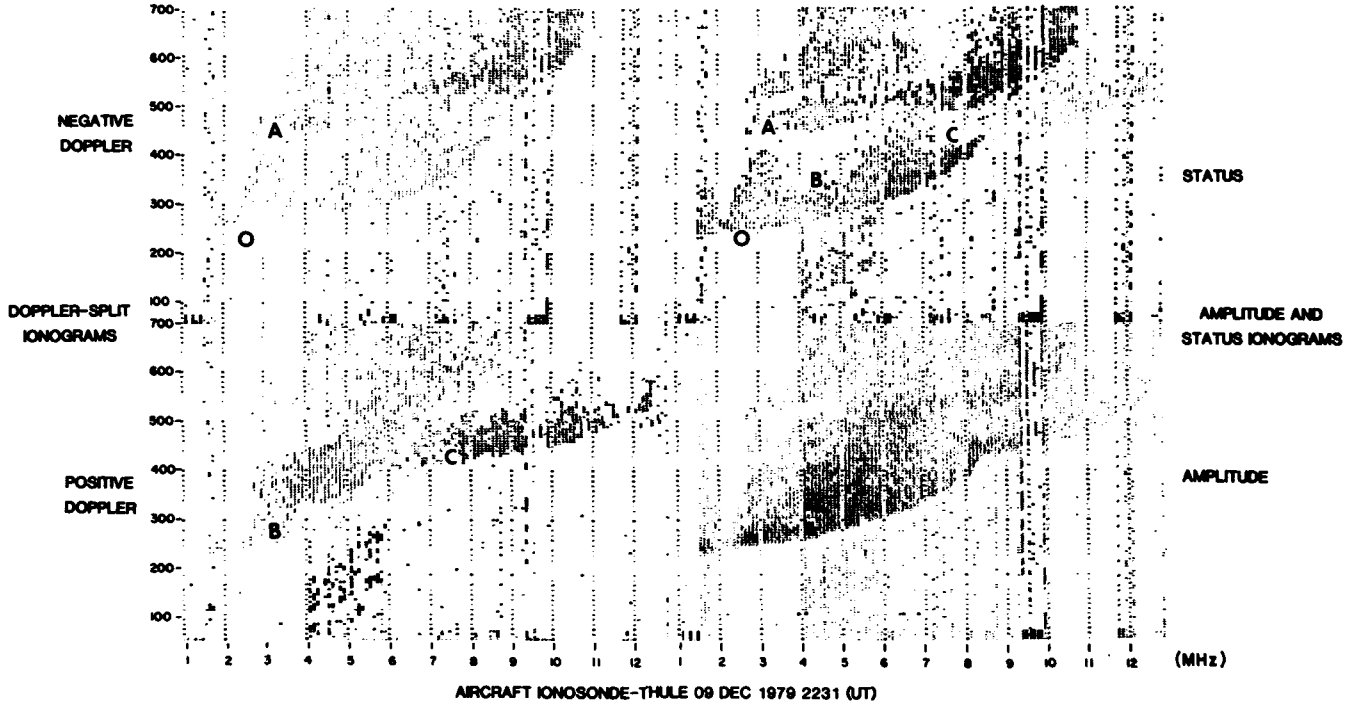

Figure 5. Typical Digital Amplitude Ionogram for Periods of Steady Arc Drift

with the Doppler shift d measured in Hz and the radar frequency f given in MHz. The ionosphere in Figure 5 is moving upward at less than 30 m/sec (upper limit). The first multiple trace in the negative Doppler ionogram (low numbers) permits an estimate of the critical frequency of the overhead ionosphere of 4.5 MHz. The three traces A (negative Doppler), B and C (positive Doppler) show that at this time two patches (B and C) of localized irregularities were approaching the station, while one (A) was moving away. Analysis of the Doppler measurements indicates that the radial velocities of structures A and C are -150 m/sec and +150 m/sec respectively. The radial velocity of the nearby irregularity (structure B) is approximately +90 m/sec. The observed Doppler variation with range will be discussed later. The retardation of the scatter traces, seen best in trace A, suggests that these patches are not merely enhancements in the irregularity structure, but also in the electron density of the surrounding medium. Estimates of the foF2 (or maximum density) of these regions made during transit through the station zenith suggests foF2 = 9 MHz, a fourfold increase in maximum electron density over the background ionization. The consistent "tagging" of the backscatter traces with the slowly changing Doppler permitted the tracking of individual regions over extended periods (>60 min). The general consistency of the tracking was possible even though the amplitudes of the structures varied substantially, and at times approaching strong traces obscured receding weak ones (or vice versa) for several ionograms. Amplitude information alone would not have allowed consistent tracking under such conditions.

Figure 6 shows the time history of the virtual height and range data, manually extracted from a sequence of more than 50 ionograms. The figure shows that during the observation period six approaching regions (A+, B, C, D, E, F) and four receding regions (A-, B', C', D') were identified. A comparison of these data with the ASIP montage (Figure 2) shows that form A is associated with the F-region aurora observed approaching from the dusk horizon from 21 to 22 UT and receding toward the dusk horizon thereafter. The A-trace measurements show the reversal time to be 22:03 UT ± 1.5 min, in excellent agreement with the ASIP data. Trace B, associated with an auroral form on the dawn horizon, was initially receding, but reversed direction simultaneously with the reversal of trace A. The approach of trace B between 2203 UT and 2240 UT tracks the approach of the leading edge of the group of arcs, arriving directly over the aircraft between 2240 and 2250 UT (Figure 2). The comparison between ASIP and sounder data shows that the ionosonde tracks ionization enhancements and irregularities associated with the drifting arcs, that they are confined to F-region heights, and that they are probably imbedded in a background ionization of about 10^5 el /cm^3.

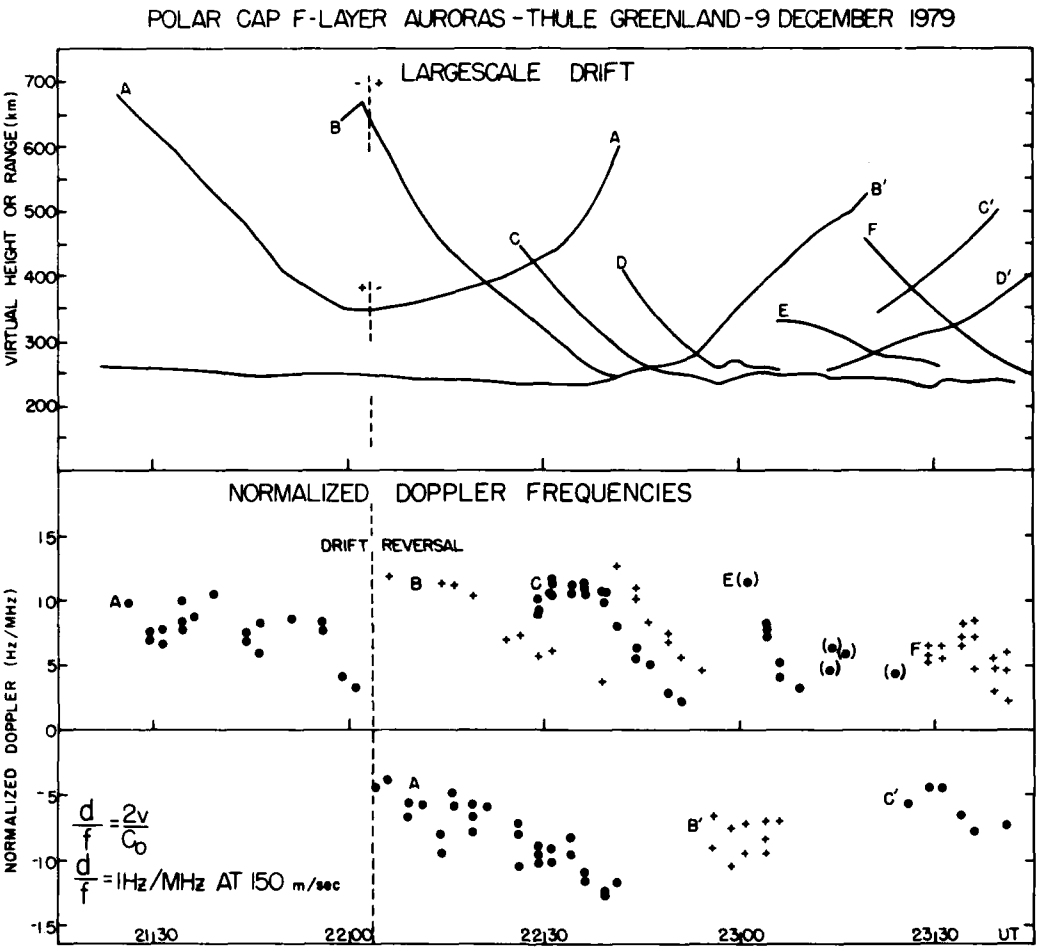

Figure 6. Time History of Virtual Height and Range Data, Extracted From a Sequence of Ionograms for a 2-h Period of Steady Arc Drift

4.2 Doppler Characteristics

Sweep frequency traces provide Doppler information as a function of frequency. Frequencies at which the discrete Doppler value changes are used to deduce the exact Doppler frequency. The bottom panel of Figure 6 presents the normalized d/f Doppler measurements. For each of the approaching forms (A through F) the Doppler is high, while the irregularity structure is at larger ranges and approaches zero as the form moves overhead. The Doppler time history of receding forms (with the exception of the clearly increasing negative Doppler of form A) is less well defined. Backscatter traces from approaching forms are usually better defined than those from receding forms. A possible difference is the irregularity

strength of the leading and trailing edges. We plan to study the irregularity generating mechanisms in the future.

Comparison of Doppler and range change measurements suggests that the returns are specular, and that the Doppler measurements give the radial velocity of an N_e enhancement moving at a height h' of about 250 km from large ranges to overhead at a generally constant horizontal velocity. The probable configuration is shown in Figure 7. To a first approximation the velocity derived from the Doppler frequency measurements changes according to

$$v_r = v \cos \alpha \tag{2}$$

where

v = horizontal velocity of arc

v_r = radial component of v

α = elevation angle to reflecting/scattering region.

Using this observation, a filter was designed to process the ionogram Doppler data automatically. The filter assumes the configuration shown in Figure 7. The observed Doppler d is (assuming optical geometry and flat earth):

$$d = \frac{2fv}{c_o} \times \sqrt{1 - (h'/r')^2} \tag{3}$$

with h' and r' the virtual height and range of the observed form and assumed to be actual height and range. To process data from forms moving at a given velocity $v_i \pm 20$ percent, the digital amplitude data are filtered by their associated Doppler frequencies using the filter:

$$v_i (1 - 0.2) < \frac{c_o \times d}{2f \sqrt{1 - (h'/r')^2}} < v_i (1 + 0.2) \tag{4}$$

The range versus time variation of the modeled configuration is also given in Figure 7. Taking the filtered amplitude data for (arbitrarily selected) velocities of 150, 250, and 400 m/sec (all using a ±20 percent velocity window), we produced virtual range characteristics. For each frequency, amplitude pixels that did not satisfy the velocity condition of Eq. (4) were set equal to zero. The ionogram is then collapsed into the height axis by summing the amplitudes for a given height bin over all frequencies and normalizing the results to the available 16-level

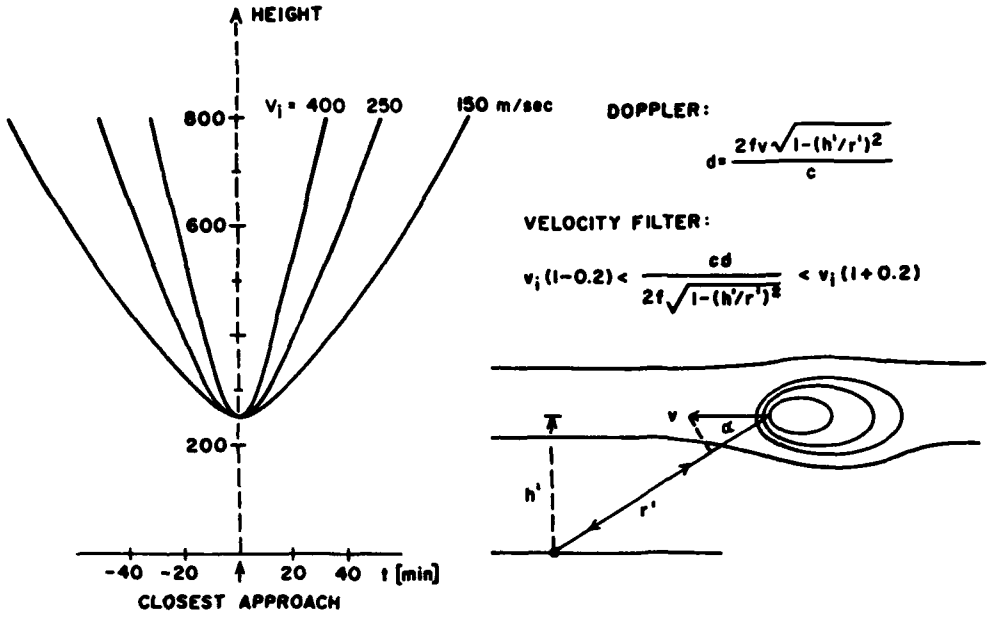

Figure 7. Range vs Time Diagram of Electron Density Enhancements Moving at Selected Horizontal Velocities. Also shown is the probable configuration of the electron density enhancement and the velocity filter applied in the data processing

printout. The range characteristics for + and - Doppler regions for the 9 December 1979 observations are shown in Figure 8. The figure shows that most of the traces moved at a velocity of about 150 m/sec. The traces identified in Figure 6 clearly appear in this automatically processed data set. Form A initially approached at a velocity very close to 150 m/sec (no evidence of any similar trace in the higher velocity windows). After the drift reversal indicated by the abrupt disappearance of form A in the positive Doppler range characteristic, form B approaches at a higher velocity as evidenced by the appearance of approaching signals in the +250 m/sec characteristic. The complexity of the propagation conditions and possible turbulence of the reflecting/scattering region broadens the Doppler spectrum enough so that the resulting traces appear at times in more than one velocity/range characteristic.

Range versus time curves developed for v = 150 and 250 m/sec using our model are superimposed (continuous lines) over traces A and B. The correspondence of the continuous lines with the characteristics confirms the general accuracy of the model.

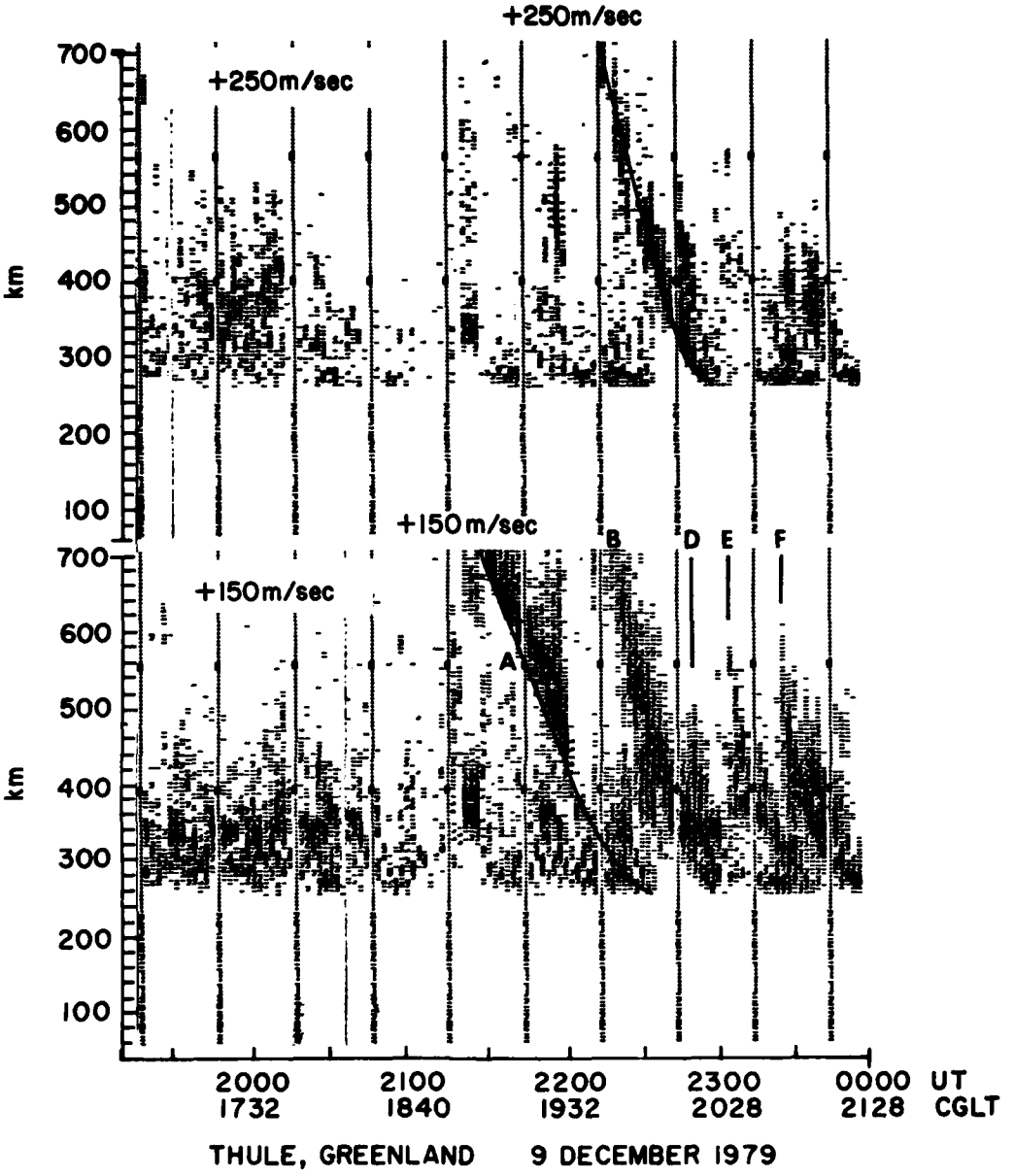

Figure 8. Range Characteristics Derived From the 9 Dec 1979 Data Set by Filtering for Velocities of +150 m/sec and +250 m/sec. It shows the acceleration of the drift starting 2215

Using the method discussed above, all 160 h of digital sounder data collected during the January 1982 campaign were transformed into range/time characteristics for the same velocity windows (150, 250 and 400 m/sec). As an example, Figure 9 covers the period 26 January 20:20 UT to 27 January 05:20 UT. The left three panels present the characteristics for approaching (+Doppler) forms, and the right three panels those for receding (-Doppler) forms. Well developed traces of auroral forms were approaching or receding from the station until 2200 UT at velocities close to 400 m/sec (best seen in the -400 m/sec panel, and at 2130 UT in the +400 m/sec panel). From 2200 to 2300 UT no traces are seen. When traces reappear after 2300 UT, they indicate velocities around 250 m/sec (positive panel), with some indication of slightly higher velocities after 0030 UT. After 0100 UT the picture becomes less well defined, with most of the energy found in the 150-250 m/sec panels except for one well defined 400 m/sec front observed arriving at 0215 UT. The remaining period (0215-0520 UT) shows (especially in the negative panels) velocities between 150 and 250 m/sec with a short burst of traces approaching at 400 m/sec around 0500 UT.

The dominant velocities derived from coarse inspection of the velocity-filtered range characteristics are given in Figure 10. Well-defined traces existed for approximately 50 percent of the time (indicated by solid arrows). Velocities could also be estimated for most for the other times, using the shift of the energy into predominantly one velocity characteristic. A good example is the period 0100 to 0130 UT in Figure 9, where most of the energy appears in the 150 m/sec panels. Periods without consistent traces are indicated by dashed arrows; times when no traces were identifiable, but substantial energy was randomly distributed in range in one specific velocity window are indicated in Figure 10 by a U at the level of the respective velocity.

The comparison of the velocity distribution with the magnetic activity index Kp shows some correlation between high velocities and high Kp. Especially, the rise to higher velocities from 12 UT on 20 January to 06 UT on 21 January and the slowing down between 22 UT on 24 January and 15 UT on 25 January parallel the observed onset and end of a geomagnetic storm period.

4.3 Drifting Patches

A somewhat different picture is observed by the ionosonde during periods when the ASIP observed antisunward drift of auroral patches. Figure 11 shows the velocity filtered range characteristics for the period 04 to 12 UT on 22 January 1982. During this period the magnetic activity peaked, with Kp = 5 for the 03 to 06 UT period. The observed traces are generally best defined in the 400 m/sec panels. A comparison with the range-versus-time curves (Figure 7) confirms that most of the fronts approach at the high velocities suggested by the high instantaneous Doppler measurements.

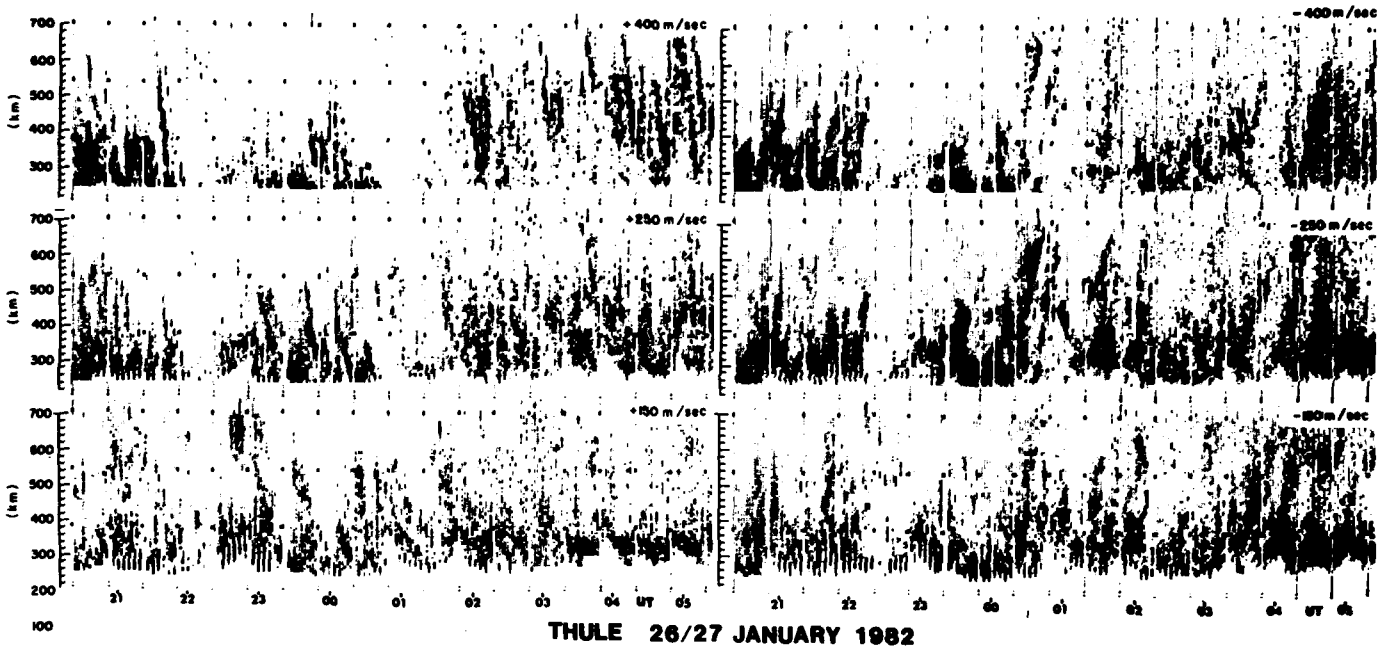

Figure 9. Velocity-Filtered Range/Time Characteristics for Velocity Windows of 150, 250, and 400 m/sec

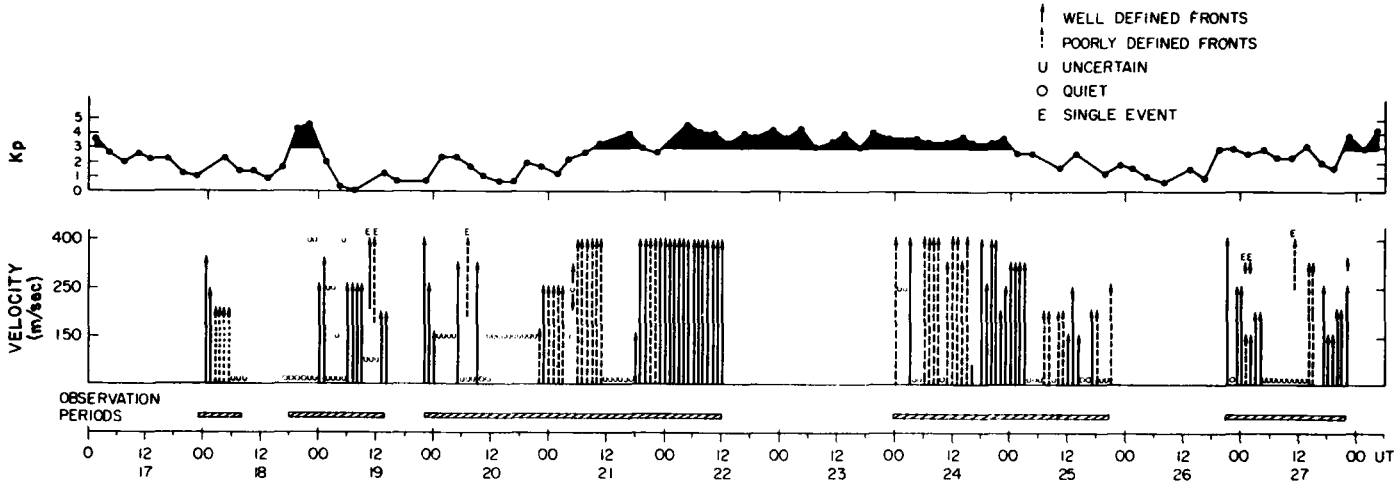

Figure 10. Predominant Velocities of Polar Cap Large Scale Irregularities From Measurements of 17 through 27 Jan 1982

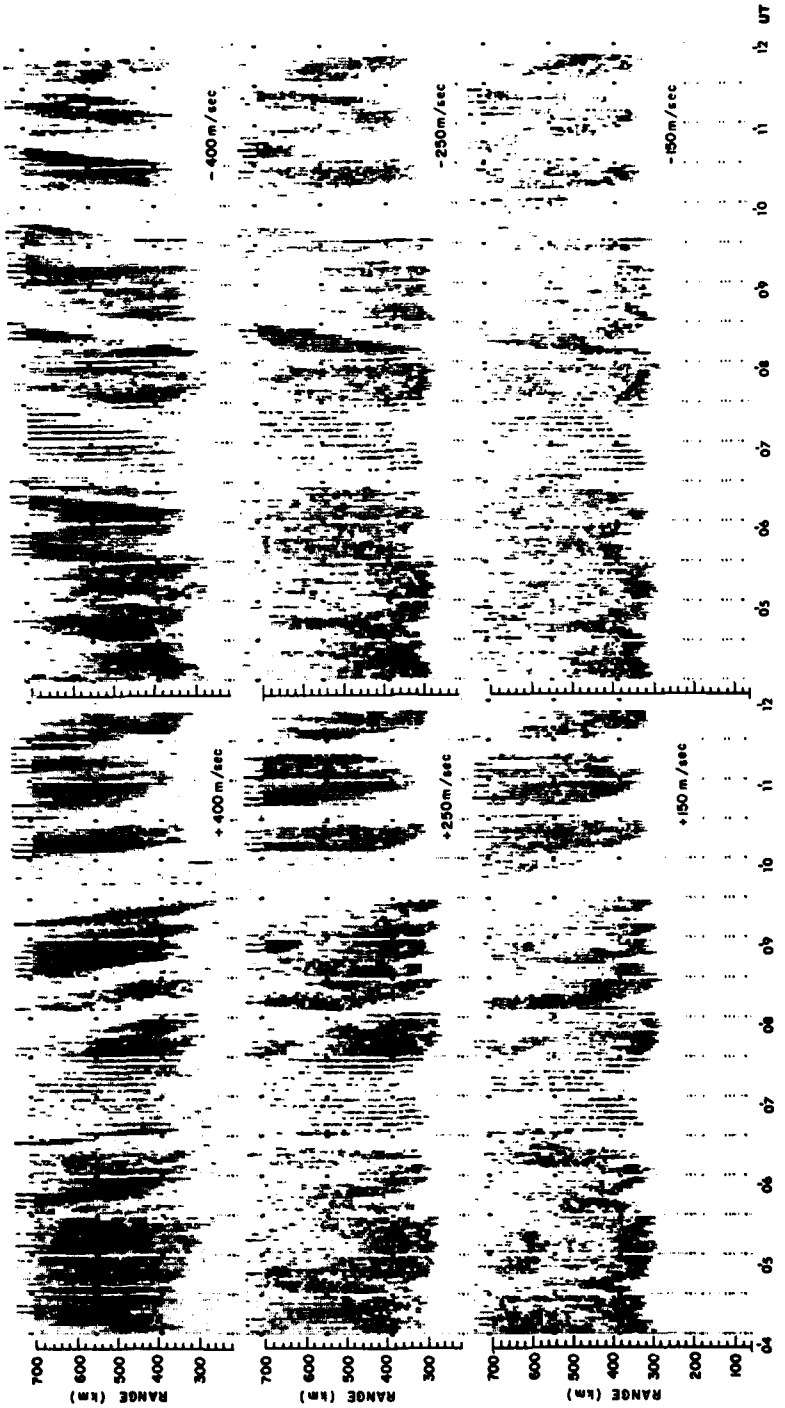

Figure 11. Velocity Filtered Range/Time Characteristics for 22 Jan 1982, During a Period of Peak Magnetic Activity, Showing Drift Velocities ≥250 m/sec

Of interest are the large range fluctuations observed especially after 0930 UT. The integrated height characteristic developed using all data irrespective of their Doppler (Figure 12) shows the same large range changes. The observed h'F (the lower at edge of the dark traces) changes by 400 km in as little as 15 min. For a period of 15 min around 10 UT ionogram traces seem to be completely absent. The sequence of selected ionograms in Figure 13 covers part of this event from 1006 to 1106 UT. The lower ionograms of each pair contain the echoes

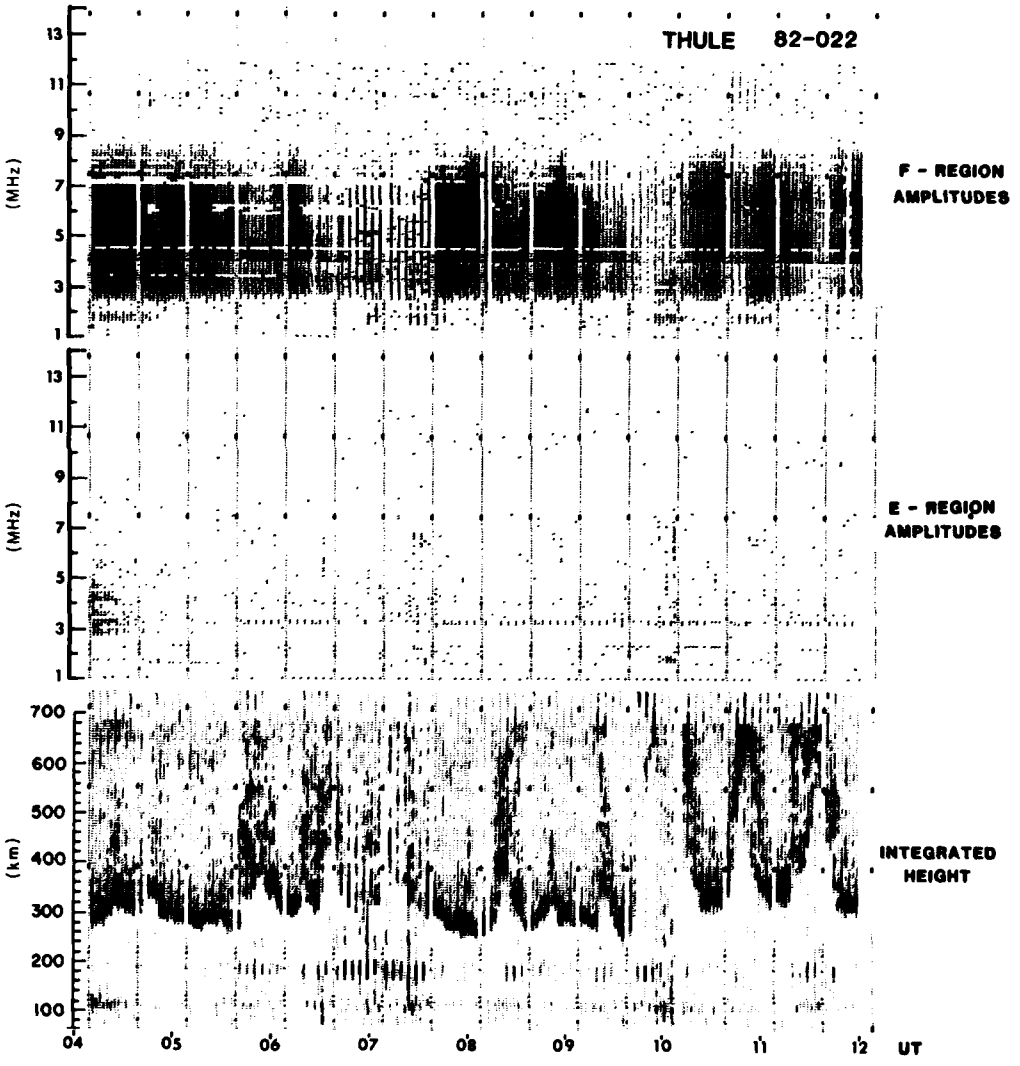

Figure 12. Virtual Height/Range Characteristics Developed Using All Data Regardless of Their Doppler for 22 Jan 1982

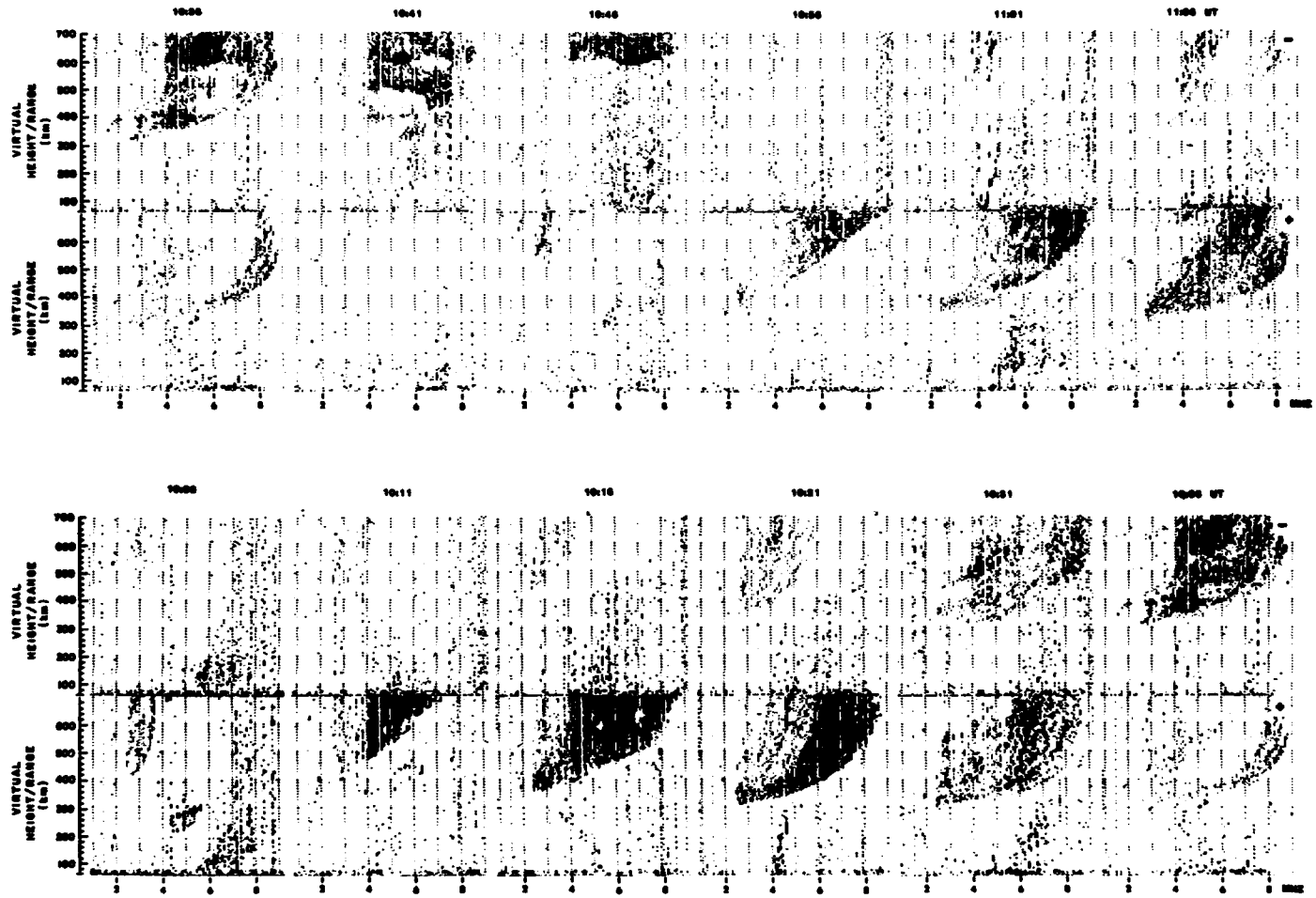

Figure 13. Sequence of Selected Ionograms From 1006 to 1106 UT, for 22 Jan 1982, Typical for Passage of a Patch Through the Zenith. The lower ionogram for each time represents amplitudes with positive, and the upper ionogram amplitudes with negative, Doppler shift

with positive, and the upper, with negative Doppler numbers. Increasing Doppler is indicated by darker numbers (larger numerical value).

The ionogram at 1006 UT shows very weak ionization overhead, with foF2 = 2.6 MHz and h'F ≈ 410 km. The few "9" values at h' = 690 km between 4.1 and 4.3 MHz are the first evidence of an approaching patch. (The high numbers at short ranges from 60 to 300 km are due to foldover of strong returns from larger ranges that are not completely eliminated by the phase coding/integration process.)

The sequence of ionograms shows the rapid approach of the front, which arrives overhead (h'F ≈ 330 km) at ~1031 UT, suggesting a horizontal velocity of close to 430 m/sec. The overhead ionogram trace at 1036 UT indicates strong enhancement of the ambient ionization to a maximum density of about 10^6 el/cm^3 (foF2 = 9.0 MHz). The patch disappeared rapidly. Precursors of the main enhancements moved away from Thule as early as 1021 UT. The ionogram at 1041 UT (after patch transit) shows only receding ionization. Low density ionization with positive Doppler is again observed at 1046 UT (foF2 = 2.8 MHz, h'F = 500 km). This is a precursor to the next patch as seen in the ionograms from 1056 to 1106 UT.

Again the retardation of the spread F traces and especially the weak trace in the negative Doppler panel at 1106 UT (foF2 ~ 8 MHz, h'F ~320 km) are evidence for substantial enhancements of background ionization within the patches.

5. CONCLUSIONS

Observations of aurora and the ionosphere over Thule using an all sky imaging photometer and a digital ionosonde have shown that three forms of aurora dominate the polar cap F-region in winter:

a. Sun-aligned arcs, drifting predominantly from dawn to dusk at speeds up to 250 m/sec extend across the whole field of view of the ASIP (>1200 km) and ~100 km in the dawn-to-dusk direction. Previous analysis[1] has shown that these arcs are produced by soft electron precipitation (<500 eV).

In the Doppler ionograms the arcs appear as spread oblique echo traces. The retardation as a function of frequency and the strong spreading observed on these traces indicate enhanced ionization as well as the presence of overdense irregularities. The rather smooth change of the observed Doppler frequencies (velocity) from initially high values to zero during the approach of the arcs is also interpreted as evidence for enhanced ionization. This localized ionization causes specular reflections with a Doppler shift proportional to the line of sight (radial) velocity rather than the horizontal velocity of the arcs. The arcs are imbedded in a background ionization with a base height of ~250 km and N_e max ≈ 10^5 el/cm^3.

b. During periods of enhanced magnetic activity (Kp = 3), large luminous patches move at speeds of between 400 and 1000 m/sec in the antisunward direction. The patches have a diffuse, cloud-like structure, and an extent of 500 to 1000 km.

A preliminary comparison with particle precipitation data obtained by the Low Altitude Plasma Instrument (LAPI) aboard the Dynamics Explorer (DE-2) satellite shows no increase in soft electron flux above the patches. (Winningham and Sharber, private communication, 1982.) The ionospheric sounder data show that fast moving patches are ionization enhancements of up to 10^6 el/cm^3, moving in a strongly depressed background ionization of less than 10^5 el/cm^3. Their origin is either the cusp region or the subcusp ionosphere. The observed 6300 Å emission is therefore airglow due to dissociative recombination of O_2^+ rather than of auroral origin.

c. At times, antisunward drift of small patches located between sun-aligned drifting arcs is observed. These small patches (<100 km extent) seem to peel off the larger arc structures. The ionograms at these times are dominated by the signatures of the F-layer arcs.

Velocity-dependent virtual range characteristics obtained using a special Doppler filter permit the survey of the large data base accumulated during 160 h of observations. Correlation of high speeds (and the likely occurrence of antisunward drifting patches) and magnetic activity is observed. An earlier observation of patches drifting in the antisunward direction out of the cusp and showing strong ($\sim 10^6$ el/cm^3) ionization enhancement was made on 26 January 1979, also under magnetically disturbed conditions (Kp = 3, ΣKp = 31+). These observations support the conclusion that antisunward convection of ionization patches is a typical polar cap feature under magnetically disturbed conditions.

References

1. Weber, E.J., and Buchau, J. (1981) Polar cap F-layer auroras, Geophys. Res. Lett. 8:125.
2. Winningham, J.D., and Sharber, J. (1982) Private communication.
3. Bibl, K., and Reinisch, B.W. (1978) The universal digital ionosonde, Radio Sci. 13:519.
4. Heelis, R.A., and Hanson, W.B. (1980) High latitude ion convection in the nighttime F region, J. Geophys. Res. 85:1995.
5. Heppner, J.P., Miller, M.L., Pongratz, M.B., Smith, G.M., Smith, L.L., Mende, S.B., and Natch, N.R. (1981) The cameo barium releases: $E_{\parallel}$ fields over the polar cap, J. Geophys. Res. 86:3519.
6. Gowell, R.W., and Whidden, R.W. (1968) Ionospheric Sounders in Aircraft, AFCRL-TR-68-0369, AD 678047.
7. Mende, S.B., Eather, R.H., and Aamodt, E.K. (1977) Instrument for the monochromatic observation of all sky auroral images, Appl. Opt. 16:1691.
8. Weber, E.J., Buchau, J., Eather, R.H., and Lloyd, J.W.F. (1977) Large-Scale Optical Mapping of the Ionosphere, AFGL-TR-77-0236, AD A051122.